

Optically transparent aromatic poly(ester imide)s with low coefficients of thermal expansion (1). Self-orientation behavior during solution casting process and substituent effect



Masatoshi Hasegawa*, Tomohiro Ishigami, Junichi Ishii

Department of Chemistry, Faculty of Science, Toho University, 2-2-1 Miyama, Funabashi, Chiba 274-8510, Japan

ARTICLE INFO

Article history:

Received 4 June 2015

Received in revised form

14 July 2015

Accepted 18 July 2015

Available online 21 July 2015

Keywords:

Poly(ester imide)

Transparency

Coefficient of thermal expansion (CTE)

Solution processability

Self-orientation

Heat-resistant plastic substrates

ABSTRACT

A series of ester-linked tetracarboxylic dianhydrides were synthesized from trimellitic anhydride chloride and hydroquinone (HQ) analogs including various alkyl substituents. The properties of aromatic poly(ester imide)s (PEsI) prepared from the tetracarboxylic dianhydrides and 2,2'-bis(trifluoromethyl) benzidine (TFMB) were investigated for applications as novel plastic substrate materials in image display devices. The chemically imidized PEsI from trimethyl-substituted HQ was soluble even in less hygroscopic solvents such as cyclopentanone (CPN). Simple casting from the CPN solution provided a flexible and less colored film with a considerably low coefficient of thermal expansion ($CTE = 11.5 \text{ ppm K}^{-1}$), a high T_g of $276 \text{ }^\circ\text{C}$, high thermal stability (5% weight loss temperature in N_2 : $453 \text{ }^\circ\text{C}$), and very suppressed water uptake ($W_A = 0.13\%$). The low CTE results from highly aligned main chains along the X - Y direction, which occurred during solvent evaporation after the PEsI solution was coated on a substrate. A mechanism is also proposed for such self-orientation behavior in this work. On the other hand, the thermally imidized counterpart was worthless in terms of low CTE and high transparency. Some conventional rigid tetracarboxylic dianhydrides were copolymerized with a minor content to di-*tert*-butyl- and diamyl-substituted PEsI systems. This approach was very effective not only for further improving some thermal properties (low CTE and high T_g) but also for suppressing film yellowness while keeping excellent solution-processability. Thus, some of the PEsIs developed in this work can be promising candidates as novel plastic substrate materials.

© 2015 Elsevier Ltd. All rights reserved.

1. Introduction

Optically transparent heat-resistant polymers are indispensable materials for applications to various optoelectronic components, e.g., plastic substrates in image display devices, liquid crystal alignment layers, color filters, optical compensation films, optical fibers, light-guiding plates, and optical lenses. One of the recent important subjects is to replace current fragile inorganic glass substrates (300–700 μm thick) in image display devices by plastic substrates (<50 μm thick), thereby the display panels can become drastically light and flexible. However, no reliable plastic substrate materials are available yet because of difficultness of simultaneously achieving high levels of required properties, i.e., optical transparency, heat resistance, dimensional stability against thermal

cycles in the device fabrication processes (thermal dimensional stability), film flexibility, and film-forming process compatibility (solution-processability). In general, plastic substrates are superior to current inorganic glass substrates in flexibility and thin-film formability but inferior in heat resistance and thermal dimensional stability.

Poly(ether sulfone) (PES) is known to possess the highest T_g ($225 \text{ }^\circ\text{C}$) among commercially available super engineering plastics. However, PES is not adapted to the present purpose in terms of short-term heat resistance (T_g) and thermal dimensional stability. Plastic substrates with poor thermal dimensional stability undergo significant thermal expansion/contraction during the multiple heating/cooling cycles in the formation processes of indium tin oxide (ITO) electrodes and thin-film transistors, which can be responsible for a serious problem such as an ITO layer breakdown.

The most reliable high-temperature polymeric materials are polyimides (PI) [1–4]. Some of aromatic PI systems also possess excellent thermal dimensional stability based on the combination

* Corresponding author.

E-mail address: mhasegaw@chem.sci.toho-u.ac.jp (M. Hasegawa).

of their much higher T_g than the device processing temperatures and the low linear coefficients of thermal expansion (CTE) along the film plane (X – Y) direction in the glassy region. However, conventional aromatic PIs show intensive coloration arising from charge-transfer (CT) interactions [5], which often disturbs their optical applications. The coloration/decoloration mechanism of aromatic PI films has been so far extensively studied from fundamental and industrial interests [5]. One of the effective approaches for the decoloration is to inhibit CT interactions by choosing non-aromatic (cycloaliphatic) monomers either in diamines or tetracarboxylic dianhydrides or both [6–16]. However, the use of cycloaliphatic monomers causes some serious problems; semi- or wholly cycloaliphatic PI films often possess poor thermal dimensional stability based on their high CTE values (>60 ppm K^{-1}) in the glassy region, even if their T_g 's were very high (>300 °C). Such high CTE arises from practically three-dimensionally random chain orientation. Most of cycloaliphatic monomers consist of non-linear/non-planar steric structures [8,9]. As a result, the overall main PI chain linearity is completely destroyed. Such distorted backbone structures do not give rise to high extents of chain alignment along the X – Y direction (called “in-plane orientation”) upon thermal imidization process [13,14,17]. Among cycloaliphatic monomers, 1,2,3,4-cyclobutanetetracarboxylic dianhydride (CBDA) and *trans*-1,4-cyclohexanediamine (*t*-CHDA) are rare cases with stiff/linear structures. However, once these monomers were used, the resulting PIs lose solution-processability. On the other hand, a wholly aromatic PI system derived from 4,4'-(hexafluoroisopropylidene) diphthalic anhydride (6FDA) and 2,2'-bis(trifluoromethyl)benzidine (TFMB) is known as a very limited case with high transparency and good solubility, although this PI film owns no low CTE characteristics, [18,19] on the basis of a non-linear/non-coplanar steric structure of the 6FDA-based diimide unit [20]. Thus, the current situation suggests how it is difficult to develop reliable plastic substrate materials with the multiple target properties.

We have previously challenged to develop solution-processable low-CTE transparent PI systems without using any cycloaliphatic monomers and reported that the combination of an amide-linked tetracarboxylic dianhydride including trifluoromethyl (CF_3) groups and TFMB led to excellent combined properties applicable to the plastic substrate materials [19]. The results motivated us to accomplish the target properties by using novel lower-cost aromatic tetracarboxylic dianhydrides without CF_3 groups, which can be prepared via a much simpler process as described later. The present work highlights aromatic poly(ester imide)s (PEIs) as the key materials. We have so far studied low-CTE PEIs with suppressed water absorption for applications as higher-performance dielectric substrates in flexible printed circuit boards (FPC) [21–23]. In this case, the PI film transparency was not a great matter of concern for FPC applications. However, we happened to be aware that the coloration of the PEI films was appreciably weaker than that of conventional aromatic PIs and amide-containing PIs [19,21]. This observation gave us an idea; an elaborate chemical modification of the PEIs may produce promising less colored high-temperature plastic substrate materials. The present work proposes a series of PEIs modified by introducing various alkyl groups and discusses a substituent effect on the target properties.

2. Experimental

2.1. Materials

2.1.1. Monomer synthesis

Ester-linked tetracarboxylic dianhydrides were synthesized from various hydroquinone analogs (HQs) and trimellitic anhydride

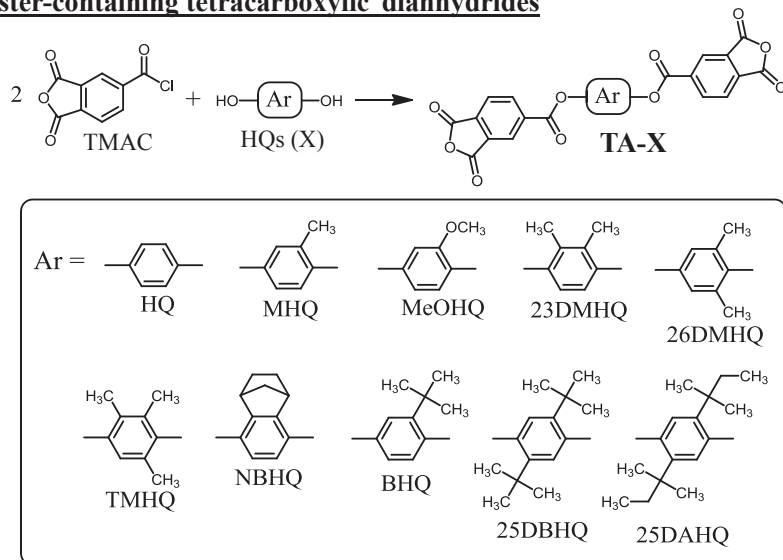
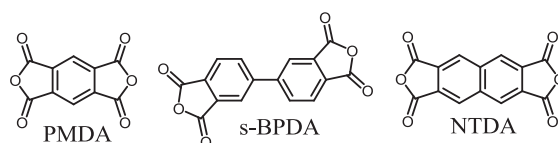
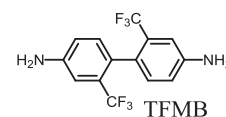
chloride (TMAC) in the presence of pyridine as an HCl acceptor in anhydrous tetrahydrofuran (THF) as described in our previous work [19], recrystallized from suitable solvents, and dried at 160 °C in vacuum for 12 h. The products were characterized by FT-IR and 1H NMR spectroscopy, elemental analysis, and differential scanning calorimetry (DSC). As a typical example, the analytical results for the product from TMAC and 2,5-di-*tert*-butylhydroquinone (25DBHQ, Fig. 1) are as follows; melting point: 325 °C (endothermic peak), FT-IR (Jasco, FT/IR 4100, KBr, cm^{-1}): 3059 (C_{arom} -H), 2959 (C_{aliph} -H), 1871/1780 (acid anhydride C=O), 1748 (ester C=O), 1487 (1,4-phenylene unit), 1H NMR [Jeol, JNM-ECP400, 400 MHz, dimethyl sulfoxide (DMSO)- d_6 , δ , ppm]: 8.70 [d, 2H, $J = 8.0$ Hz, 6,6'-protons of phthalic anhydride (PA)], 8.61 (s, 2H, 3,3'-protons of PA), 8.33 (d, 2H, $J = 8.0$ Hz, 5,5'-protons of PA), 7.41 (s, 2H, central disubstituted phenylene), 1.30 (s, 18H, *tert*-butyl group). Anal. Calcd (%) for $C_{32}H_{26}O_{10}$ (570.54): C, 67.36; H, 4.59. Found: C, 67.19; H, 4.59. An analog from trimethyl-substituted HQ (TMHQ, Fig. 1) was also synthesized and characterized in a similar manner; FT-IR (KBr, cm^{-1}): 3109 (C_{arom} -H), 2933 (C_{aliph} -H), (1857/1782 (acid anhydride C=O), 1735 (ester C=O), 1480 (1,4-phenylene unit), 1H NMR (DMSO- d_6 , δ , ppm): 8.76–8.65 (m, 4H, 3,3',6,6'-protons of PA), 8.33–8.30 (m, 2H, 5,5'-protons of PA), 7.23 (s, 1H, central tri-substituted phenylene), 2.16–2.09 (m, 9H, CH_3). Anal. Calcd (%) for $C_{27}H_{16}O_{10}$ (500.41): C, 64.80; H, 3.22. Found: C, 64.64; H, 3.27. Other relevant monomers were also synthesized in a similar manner. In this work, the ester-containing tetracarboxylic dianhydrides were designated as TA-X ($X =$ hydroquinone analogs), e.g., “TA-TMHQ” in case of $X =$ trimethylhydroquinone (TMHQ).

2.1.2. Polyaddition, imidization, and film preparation

The sources, purification methods, and melting points of monomers and raw materials are summarized in [Supplementary data 1](#). PEI precursors [poly(amic acid)s (PAA)] were prepared by equimolar polyaddition of tetracarboxylic dianhydrides and diamines in dry *N,N*-dimethylacetamide (DMAc) as described in our previous papers [13–16,19]. The reaction scheme is shown in Fig. 2. The formation of PAAs was confirmed from the transmission-mode FT-IR spectra recorded on an FT/IR 4100 infrared spectrometer (Jasco) using separately prepared thin cast films (4–6 μm thick) with a non-uniform thickness to erase interference fringes. A typical FT-IR spectrum is depicted in Fig. 3(a). Some specific bands (cm^{-1}) are observed: 3259 (amide, N-H), 3057 (C_{arom} -H), 2969/2878 (C_{aliph} -H), 2630 (hydrogen-bonded COOH, O-H), 1735 (ester, C=O), 1687/1534 (amide, C=O), 1490 (1,4-phenylene unit), and 1323 (CF_3 , C-F).

The PAAs were converted to PEIs by different methods (thermal and chemical imidization) (Fig. 2). When the imidized forms were highly soluble, PAAs were chemically imidized as previously described [14,16,19]. The imidized samples isolated as fibrous white precipitates were re-dissolved in a fresh anhydrous solvent [e.g., cyclopentanone (CPN), triglyme (Tri-GL), or DMAc] at a solid content of 5–15 wt%. The homogeneous PEI solutions were coated on a glass substrate and dried typically at 60 °C for 2 h in an air convection oven and successively heated typically at 250 °C for 1 h in vacuum on the substrate. After peeling them off from the substrate, the PEI films (typically 20 μm thick) were annealed typically at 255 °C/1 h in vacuum to remove residual stress. The thermal conditions were properly adjusted for obtaining better quality of films. The samples prepared via chemical imidization are denoted as “(C)” from now on.

PEI films were also prepared upon thermal imidization; PAA solution was bar-coated on a glass substrate, dried at 60 °C for 2 h in an air-convection oven, and heated typically at 200 °C/0.5 h + 350 °C/1 h in vacuum on the substrate, and successively annealed in vacuum at 10–20 °C lower temperatures than the T_g

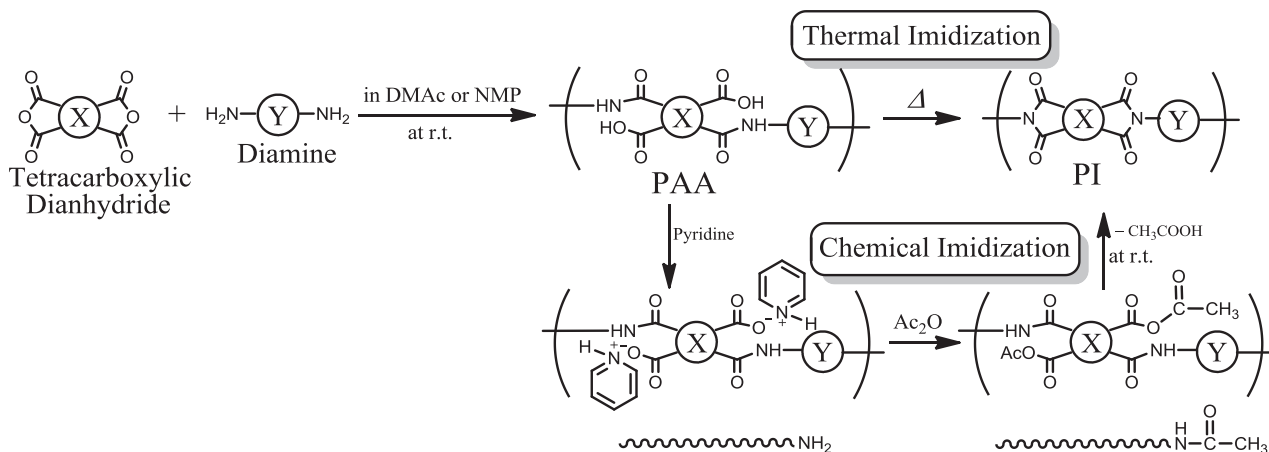
Ester-containing tetracarboxylic dianhydrides**Tetracarboxylic dianhydrides (Comonomers)****Diamine****Fig. 1.** Structures of ester-containing tetracarboxylic dianhydrides and comonomers.

without the substrate to eliminate residual stress. The imidization and annealing conditions were properly adjusted to form better quality of PEI films. In this work, the thermally imidized film samples are represented as “(T)” from now on.

For soluble PEI systems, the completion of imidization was confirmed from perfect disappearance of the proton signals for the NHCO [$\delta \sim 10.0$ ppm in DMSO- d_6] and the COOH groups ($\delta = 12\text{--}13$ ppm) in the ^1H NMR spectra. Full imidization was also confirmed from the FT-IR spectra of the separately prepared thin films. Fig. 3(b) displays a typical FT-IR spectrum of a thin film prepared by solution casting of a chemically imidized powder sample. In addition of complete disappearance of the PAA-inherent

infrared bands, the appearance of some imide specific bands (cm^{-1}) are observed: 3074 ($\text{C}_{\text{arom}}\text{-H}$), 2969/2879 ($\text{C}_{\text{aliph}}\text{-H}$), 1786 (imide-I, $\text{C}=\text{O}$), 1734 (imide-II + ester, $\text{C}=\text{O}$), 1492 (1,4-phenylene unit), 1372 (imide-III, $\text{N}-\text{C}_{\text{arom}}$), 1310 (CF_3 , $\text{C}-\text{F}$), and 724 (imide-IV, ring deformation). All other thermally imidized films also showed similar spectral features, suggesting complete imidization.

In this work, the chemical compositions of PAA and PEI systems are represented by means of monomer abbreviations [tetracarboxylic dianhydrides (A) and diamines (B)] as A/B for homopolymers and $\text{A}_1;\text{A}_2/\text{B}$ for copolymers.

**Fig. 2.** Reaction schemes of polyaddition and imidization of poly(amic acid)s, and expected end-capping of the terminal amino groups during chemical imidization.

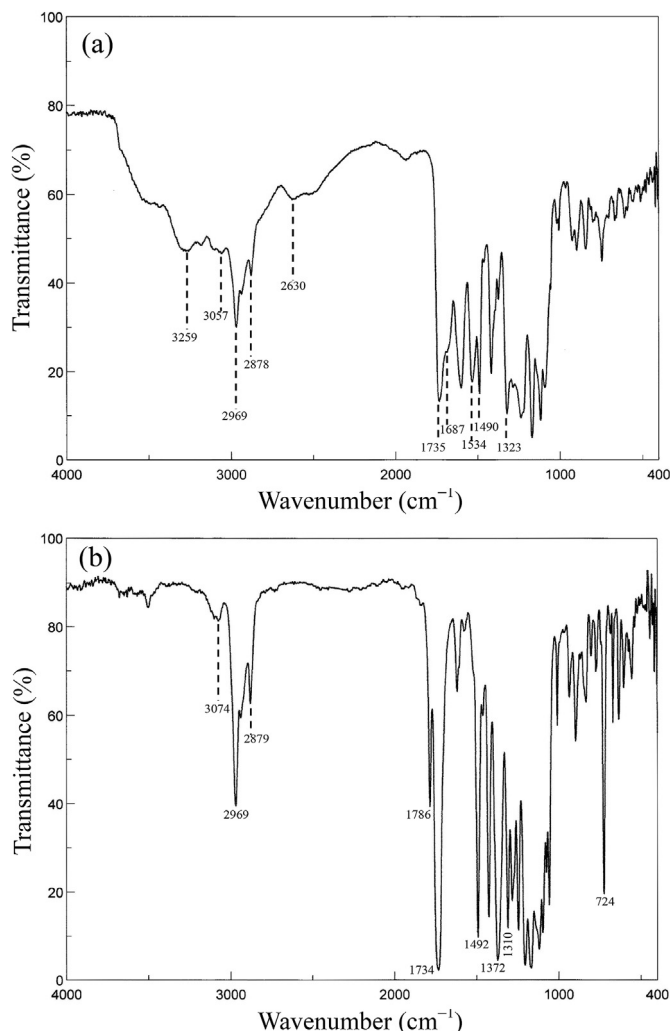


Fig. 3. FT-IR spectra of thin films for TA-25DAHQ/TFMB system: (a) PAA and (b) PI.

2.2. Measurements

2.2.1. Inherent viscosity and molecular weight

The reduced viscosities (η_{red}) of PAAs, which can be practically regarded as η_{inh} , were measured in DMAc at a solid content of 0.5 wt% at 30 °C on an Ostwald viscometer. The number- (M_n) and weight-average molecular weights (M_w) for PEIs were determined by the gel permeation chromatography (GPC) using THF as an eluent at room temperature on a Jasco, LC-2000 Plus HPLC system with a GPC column (Shodex, KF-806L) at a flow rate of 1 mL min⁻¹ by ultraviolet–visible detection at 300 nm (Jasco, UV-2075). The calibration was carried out using standard polystyrenes (Shodex, SM-105).

2.2.2. Linear coefficient of thermal expansion

The CTE along the film plane (X–Y) direction for PEI specimens (15 mm long, 5 mm wide, and typically 20 μ m thick) in the glassy region were measured by the thermomechanical analysis (TMA) as an average in the range of 100–200 °C at a heating rate of 5 °C min⁻¹ on a thermomechanical analyzer (Netzsch, TMA 4000) with a fixed load (0.5 g per a unit film thickness in μ m, typically, 10 g load for 20 μ m-thick films) in a dry nitrogen atmosphere. In this case, after the preliminary first heating run up to 120 °C and successive cooling to room temperature in the TMA chamber, the data

were collected from the second heating run for removing an influence of adsorbed water.

2.2.3. Glass transition temperature

The storage modulus (E') and the loss energy (E'') of PEI films were measured by the dynamic mechanical analysis (DMA) at a heating rate of 5 °C min⁻¹ on the same TMA instrument. The measurements were conducted at a sinusoidal load frequency of 0.1 Hz with an amplitude of 15 gf in a nitrogen atmosphere. The T_g of PEI films was determined from a peak temperature of the E'' curve (method-1). The T_g was also determined from an inflection point of the TMA curve, where the specimens started to abruptly elongate under a fixed load, as an intersection of two tangential lines (method-2).

2.2.4. Optical properties

The light transmission spectra of PEI films (typically 20 μ m thick) were recorded on an ultraviolet–visible spectrophotometer (Jasco, V-530) in the wavelength (λ) range of 200–800 nm. The light transmittance at 400 nm (T_{400}) and the cut-off wavelength (λ_{cut}) where the transmittance becomes practically null were determined from the spectra. The yellowness indices (YI, ASTM E 313) for PEI films were also determined from the spectra under a standard illuminant of D65 and a standard observer function of 2° on a color calculation software (Jasco) on the basis of the relation:

$$YI = 100(1.2985x - 1.1335z)/y$$

where x , y , and z are the CIE tristimulus values. YI takes zero for an ideal white/transparent sample. The total light transmittance (T_{tot} , JIS K 7361-1) and the diffuse transmittance (T_{diff} , JIS K 7136) of PEI films were measured on a double-beam haze meter equipped with an integrating sphere (Nippon Denshoku Industries, NDH 4000). The haze (turbidity) of PEI films was calculated from the relation:

$$\text{Haze} = \left(T_{diff} / T_{tot} \right) \times 100$$

The in-plane (n_{in} or n_{xy}) and out-of-plane (n_{out} or n_z) refractive indices of PEI films were measured with a sodium lamp at 589.3 nm (D-line) on an Abbe refractometer (Atago, 4T, n_D range: 1.47–1.87) equipped with a polarizer by using a contact liquid (sulfur-saturated methylene iodide, $n_D = 1.78$ –1.80) and a test piece ($n_D = 1.92$). The birefringence of PEI films, which stands for a relative extent of chain alignment along the X–Y direction, was calculated from the relation:

$$\Delta n_{th} = n_{in} - n_{out}$$

2.2.5. Mechanical properties

The tensile modulus (E), tensile strength (σ_b), and elongation at break (ϵ_b) of PEI specimens (film dimension: 30 mm long, 3 mm wide, typically 20 μ m thick, specimen numbers > 15) were measured on a mechanical testing machine (A & D, Tensilon UTM-II) at a cross head speed of 8 mm min⁻¹ at room temperature. The specimens were cut off from high-quality film samples (10 cm \times 10 cm) without any defects such as fine bubbles. The data analysis was carried out on a data processing program (Softbrain, UtpAcS Ver. 4.09).

The measurements for the other properties [thermal stability (5% weight loss temperature, T_5^w), extent of water absorption (W_A), solubility, and wide-angle X-ray diffraction) were also conducted as previously described [16,19].

3. Results and discussion

3.1. Molecular design

The PI properties are primarily governed by the structures of monomers chosen. Taking into account our goal (to simultaneously achieve low CTE, high transparency, excellent solution-processability, and sufficient film flexibility), the suitable diamine monomers are practically limited to TFMB. A rod-like structure as seen typically in TFMB is indispensable for low CTE generation. The electron-withdrawing CF_3 groups of TFMB contribute to a blue-shift of the intramolecular CT absorption band, as a result, a decrease in the film coloration [5]. The bulky CF_3 groups with extremely low polarizability are also valid for disturbing dense interchain stacking and crystallization, as a result, they are often effective for solubility improvement. The position of the CF_3 substituents also affects the solubility; it is most likely that TFMB consists of a distorted (non-coplanar) biphenylene structure owing to steric hindrance between the 2,2'-substituted CF_3 groups and the 6,6'-hydrogen atoms [24]. The expected loose chain stacking is also advantageous for reducing intermolecular CT interactions as a secondary factor of film coloration [5]. The replacement of the CF_3 groups in TFMB by CH_3 groups (use of *m*-tolidine) inevitably causes intensive coloration because of a decrease in the electron-withdrawing ability. An isomer of TFMB, 3,3'- CF_3 -substituted counterpart is probably inferior to TFMB in the polymerization reactivity with tetracarboxylic dianhydrides by a steric hindrance effect of the 3,3'- CF_3 groups adjacent to the functional amino groups.

The success of this work depends on the molecular design of tetracarboxylic dianhydride monomers. Fig. 4 illustrates an impact of para/meta isomerism at the diimide units on CTE. Here, the diamine component is fixed to TFMB or *p*-PDA with linear structures. In fact, the rod-like or all para-linked PI systems [Fig. 4(a)–(c)] have much lower CTE values than the isomeric systems with distorted backbone structures [(d)–(f)]. The results imply how the “overall” main chain rigidity/linearity is important for deriving low CTE characteristics. This means that not only the diamines but also the tetracarboxylic dianhydrides should possess rigid/linear structures. However, as far as conventional rigid aromatic tetracarboxylic dianhydrides [typically, pyromellitic

dianhydride (PMDA)] are used for lowering the CTE, it is usually inevitable to deteriorate other desired properties (e.g., film transparency and solution-processability). As illustrated in Supplementary data 2, previous studies revealed that structural modifications by introducing CF_3 groups into conventional rigid tetracarboxylic dianhydrides [PMDA and 3,3',4,4'-biphenyl/tetracarboxylic dianhydride (*s*-BPDA)] were effective for improving some focused properties (typically, dielectric constant) while keeping low CTE characteristics, although the PI film transparency was not always the target in these attempts [25,26]. 3,3',4,4'-*p*-Terphenyltetracarboxylic dianhydride (TPDA) [27–29] and 2,3,6,7-naphthalenetetracarboxylic dianhydride (NTDA) [17] are also known as conventional rigid aromatic tetracarboxylic dianhydrides profitable for low CTE generation. However, there are so far no reports where these monomers were modified with some substituents probably owing to a synthetic problem. On the other hand, TA-HQ can be modified much more flexibly because various substituted HQs are commercially available as the raw materials. Thus, it is possible to widely vary the intermolecular forces upon this approach while retaining the rigid structure inherent to TA-HQ.

3.2. Properties of homo PEIs

3.2.1. PEIs from non- and mono-substituted TA-HQs

We have previously reported the thermal and mechanical properties of thermally imidized PEI films prepared from TFMB with non-substituted and methyl/methoxy-substituted TA-HQs without interests on the film transparency [22]. Then we began on evaluating the film transparency of these systems as the first step of the present work. The properties are listed in Table 1. Regardless of the substituents, the TA-HQ analogs showed sufficiently high reactivity with TFMB to form high molecular weights of PAAs with $\eta_{\text{inh}} > 2 \text{ dL g}^{-1}$, which is much higher than an empirical criterion for sufficient film-forming ability ($\eta_{\text{inh}} \sim 1 \text{ dL g}^{-1}$). The high η_{inh} values were also maintained after chemical imidization as in the other substituted TA-HQs/TFMB systems, corresponding to actual high molecular weights [e.g., $\eta_{\text{inh}} = 5.20 \text{ dL g}^{-1}$, $M_n = 9.56 \times 10^4$, $M_w = 2.19 \times 10^5$ for the chemically imidized TA-25DAHQ/TFMB powder sample]. The chemical imidization process compatibility could be the key to our goal because PI films prepared via this

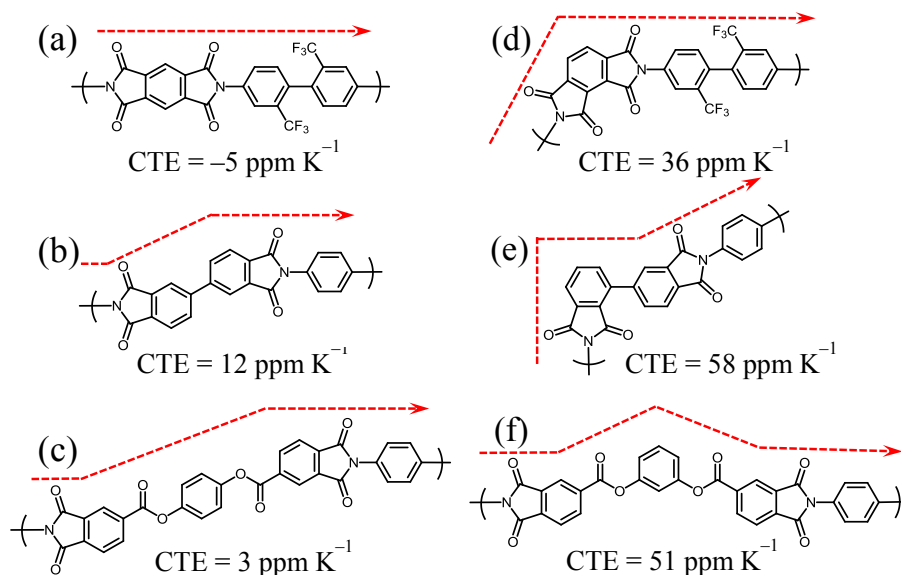


Fig. 4. Impact of overall chain linearity on CTE: (a–c) PIs derived from conventional rigid tetracarboxylic dianhydrides with rod-like diamines and (d–f) the counterparts from the distorted tetracarboxylic dianhydride isomers. The broken arrows stand for main chain linearity.

Table 1
Film properties of homo PEIs derived from TFMB with non-/mono-substituted TA-HQs.

Tetracarboxylic dianhydride	η_{inh} (dL g ⁻¹)	Cure ^c	Solvent ^d (PI content)	Appearance of PI films	T_{400} (%)	λ_{cut} (nm)	CTE (ppm K ⁻¹)
TA-HQ	2.93 ^a	T	–	Slightly turbid	54.0	354	23.2
TA-MHQ	3.79 ^a	T	–	Turbid	13.4	365	20.3
	4.64 ^a	C	NMP (7 wt%)				
TA-MeOHQ	1.23 ^b	T	–	Turbid	1.3	394	34.0
	3.87 ^a						
	5.96 ^a						
	2.63 ^b						

^a Data for PAA solutions just after polymerization.

^b Data for chemically imidized powder samples.

^c Cure (imidization) processes. T: thermal imidization, C: chemical imidization in homogeneous solution.

^d Solvents for re-dissolution of chemically imidized powder samples.

process tend to display appreciably better properties (higher transparency and lower CTE) than the counterparts via the conventional two-step process (thermal imidization of PAA films) as discussed later [14,16,19]. The non-substituted TA-HQ/TFMB system was not meet for the chemical imidization process because of gelation based on poor solubility of the imidized form, which disturbs full imidization. On the other hand, a positive effect of the substituents (–CH₃ and –OCH₃) was observed; the solution homogeneity was kept during chemical imidization. In fact, the chemically imidized powder sample (C) for TA-MHQ/TFMB was soluble only in hot amide solvents [*N,N*-dimethylformamide (DMF), DMAc, and *N*-methyl-2-pyrrolidone (NMP)] at a solid content of 1 wt%. The methoxy-substituted counterpart owned improved solubility; it was soluble even in hot non-amide solvents [γ -butyrolactone (GBL), DMSO, *m*-cresol, and CPN] in addition to common amide solvents. The chemical imidization process compatibility also brought about another merit: an appreciably decreased CTE (15.5 ppm K⁻¹) for TA-MeOHQ/TFMB. However, the use of these mono-substituted TA-HQs also caused a significant decrease in the film transparency (T_{400}) as listed in Table 1. In particular, the methoxy-substituted system is beyond the present candidates owing to its film coloration, which is probably related to initial coloration of TA-MeOHQ monomer. The incorporation of the methyl group to TA-HQ/TFMB also seems to somewhat decrease the film transparency. However, the magnitude of a λ_{cut} -based spectral red-shift by introducing the singular methyl group to TA-HQ/TFMB ($\Delta\lambda_{cut} = 11$ nm) was much lower than that by the incorporation of the methoxy group ($\Delta\lambda_{cut} = 40$ nm). The results motivated us to investigate how plural methyl substituents influence the film transparency, solubility, and the other target properties.

3.2.2. PEIs from multi-methyl-substituted TA-HQs

As the next step, we investigated how the position/number of the methyl groups influences the target properties with expectation of property improvement. The properties are summarized in Table 2. Unexpectedly, the introduction of an additional methyl group to TA-MHQ, i.e., the 2,3-dimethyl substitution destroyed the chemical imidization process compatibility because of gelation. Thermal imidization of the corresponding PAA film led to a highly hazy and colored PEI film, although it maintained a still relatively low CTE (~40 ppm K⁻¹). Similarly to non-substituted TA-HQ/TFMB, the TA-23DMHQ/TFMB PEI film (T) displayed double thermal transition behavior with the E'' peaks at 340 °C (T_g) and 212 °C (probably sub- T_g) in the DMA curve. In some PEI systems, sub- T_g appears distinctly around 210–230 °C in the DMA curves [30]. Compared to DMA, TMA is often insensitive to sub- T_g , so that only T_g can be detected as an inflection point corresponding to a softening temperature in the TMA curves. Actually, a single transition (only T_g) was observed at 358 °C for this PEI film (T) by TMA. The film properties of TA-23DMHQ/TFMB indicate that this system is not

valuable to our aim. On the other hand, the use of the dimethyl-substituted isomer at different positions (TA-26DMHQ) enabled us to perform chemical imidization in a homogeneous state. In this system, the film transparency (T_{400}) was significantly improved just by altering the imidization route from thermal to chemical process as shown in Table 2. The chemical imidization process was also more profitable for decreasing CTE than thermal imidization as observed in the TA-MeOHQ/TFMB system.

Trimethyl-substituted TA-TMHQ, which corresponds to a combined structure of 2,3- and 2,6-dimethyl-substituted monomers, was used as the next approach. The thermally imidized PEI film possessed no remarkable properties; poor transparency and a common level of CTE (>50 ppm K⁻¹). On the other hand, in spite of the same chemical composition, the DMAc-cast PEI film (C) achieved excellent combined properties: drastically enhanced transparency ($T_{400} = 61.7\%$), a very low CTE (13.4 ppm K⁻¹), a high tensile modulus (5.7 GPa), sufficient film flexibility ($\epsilon_b^{max} = 14\%$), and high thermal stability ($T_d^5 > 450$ °C in N₂). This PEI film (C) possessed a single thermal transition (T_g) irrespectively of the analytical methods: at 261 °C by DMA (275 °C by TMA). The low CTE and the high tensile modulus are closely related to a high extent of in-plane chain orientation in accordance with a high level of the Z-direction birefringence ($\Delta n_{th} \sim 0.1$) as demonstrated from good correlations (Δn_{th} vs. CTE and modulus) in Fig. 5. Table 2 also reveals that the use of CPN (b.p. 131 °C) as a casting solvent instead of DMAc (b.p. 165 °C) was appreciably effective to improve the film transparency. In our experience, less volatile amide solvents such as NMP (b.p. 202 °C) are unfavorable from the viewpoint of the film transparency. Such extra coloration as observed in NMP-cast PEI films may originate from a trace amount of a thermally decomposed NMP residue. The CPN-cast PEI film (C) for TA-TMHQ/TFMB also displayed a further decreased CTE as listed in Table 2. The predominance of the chemical imidization process is undoubted from Fig. 6 [chemical imidization (Y-axis) vs. thermal imidization (X-axis) for the present systems]; the comparison for CTE revealed that the data points are basically located below the $Y = X$ line where the CTE values do not depend on the imidization methods at all, and those for T_{400} are all positioned from the $Y = X$ line upward. The suppressed coloration of the PEI films (C) is probably attributed to not only the film formation process at much lower temperatures than for thermal imidization but also an end-capping reaction of the thermally unstable terminal amino groups by Ac₂O during chemical imidization as depicted in Fig. 2. The control of film turbidity is also an important subject. As mentioned above, the PEI systems derived from TFMB with non-, mono-, and di-substituted TAHQs led to rather hazy films irrespectively of the imidization pathways. On the other hand, the combination of the use of trimethyl-substituted TA-TMHQ and chemical imidization allowed the formation of a completely clear PEI film with a very low haze value of 1.48% in contrast to the thermally imidized counterpart. Both of the

Table 2
Film properties of homo PEIs derived from TFMB with di-/trimethyl-substituted TA-HQs.

Tetracarboxylic dianhydride	η_{inh} (dL g ⁻¹)	Cure	Solvent (PI content)	Appearance of PI films	T_{400} (%)	λ_{cut} (nm)	Δn_{th}	$T_g/sub-T_g^f$ (°C)	CTE (ppm K ⁻¹)	E (GPa)	ϵ_b ave/max (%)	σ_b (GPa)	T_d^5 (N ₂) (°C)	T_d^5 (air) (°C)
TA-23DMHQ	2.39 ^a	T		Highly turbid	0	432	— ^c	340/212 ^d	42.6	3.43	6/7	0.10	461	422
TA-26DMHQ	0.64 ^a	T		Turbid	0		— ^c	358/— ^e	80.5	3.37	40/46	0.11	450	429
	0.95 ^b	C	CPN (11 wt%)	Slightly Turbid	39.5	359	0.069	292/240 ^e	49.3	4.04	5/7	0.11	464	443
TA-TMHQ	4.28 ^a	T		Turbid	0	433	— ^c	—/217 ^d	54.3				453	414
	4.28 ^a	C	DMAc (7.3 wt%)	Clear	61.7	360	0.096	261/— ^d	13.4	5.70	8/14	0.19	454	414
	6.57 ^b							275/— ^e						
	5.80 ^a	C	CPN (5.0 wt%)	Clear	64.8	358	0.113	257/— ^d	11.5	5.50	15/27	0.22	453	419
	8.44 ^b							276/— ^e						

^a Data for PAA solutions just after polymerization.

^b Data for chemically imidized powder samples. For chemical imidization, the same PAA as that for thermal imidization was used unless the data for PAA was indicated in the cell.

^c The refractive index measurements were difficult because of intensive turbidity.

^d Data determined by DMA (method-1).

^e Data determined by TMA (method-2).

^f Blank data mean that the transitions were not detected by the measurements.

turbid (T) and the clear PEI film (C) for TA-TMHQ/TFMB are regarded as being non-crystalline on the basis of a broad halo in the WAXD pattern, as well as the turbid films of the other systems. Thus, crystallization is not responsible for the film turbidity observed here. The CPN-cast TA-TMHQ/TFMB film also possessed a very low extent of water absorption ($W_A = 0.13\%$) as another feature.

3.2.3. PEIs from TA-HQs with bulkier side groups

Some side groups bulkier than the methyl substituent were also incorporated into TA-HQ/TFMB. Table 3 summarizes the film properties. TA-NBHQ including an HQ-norbornane fused-ring structure provided less valuable properties as judged from its poor

light transparency and a high CTE value even when the film was prepared via chemical imidization. The results might reflect that the norbornane side group was too bulky to promote the casting-induced in-plane orientation behavior responsible for low CTE characteristics. If that is the case, further investigations by incorporating other bulkier substituents seem to be hopeless for aiming at the present goal.

A thermally imidized PEI film obtained from mono-*tert*-butyl-substituted TA-BHQ and TFMB also gave some disappointing results without remarkable properties except for a rather high ϵ_b^{\max} value. On the other hand, a specific substituent effect on CTE was observed when the TA-BHQ/TFMB film was prepared via chemical

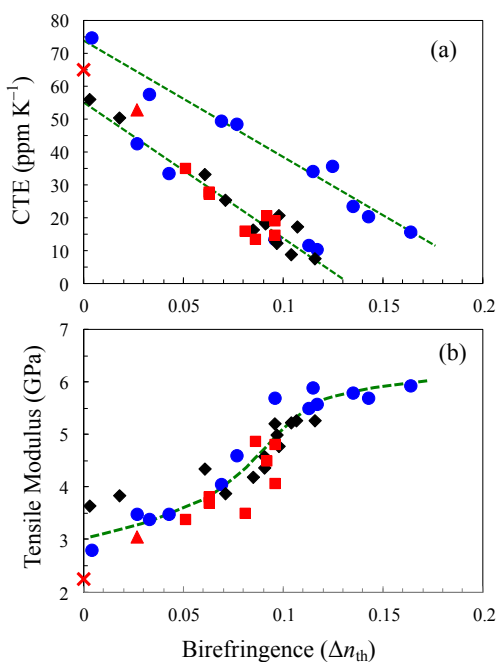


Fig. 5. Relationships between birefringence (Δn_{th}) and some properties: (a) CTE and (b) tensile modulus. (●) TA-HQs/TFMB homo PEIs, (◆) TA-25DBHQ/TFMB-based co-PEIs, (■) TA-25DAHQ/TFMB-based co-PEIs, (▲) chemically imidized 6FDA/TFMB and (×) PES.

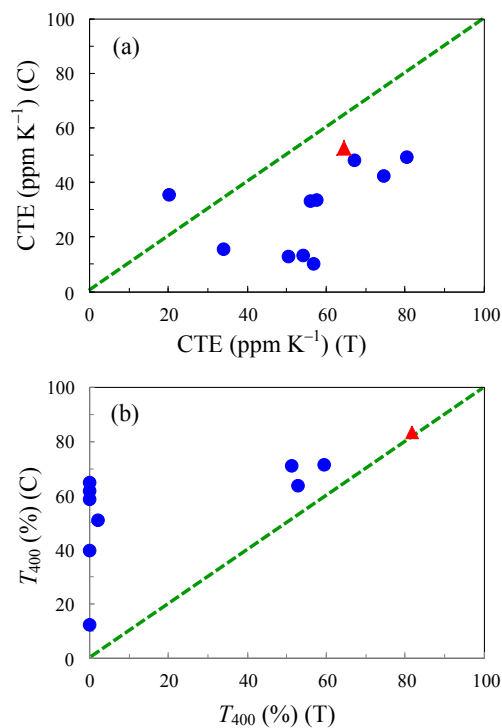


Fig. 6. Effects of imidization method on some properties: (a) CTE and (b) light transmittance at 400 nm (T_{400}). (●) TA-HQs/TFMB homo and copolymer systems and (▲) 6FDA/TFMB. The dotted line denotes the relation: $Y = X$.

Table 3
Film properties of homo PEIs derived from TFMB with TA-HQs containing bulky groups.

Tetracarboxylic dianhydride	η_{inh} (dL g ⁻¹)	Cure	Solvent (PI content)	Appearance of PI films	T_{400} (%)	λ_{cut} (nm)	Δn_{th}	T_g (°C)	CTE (ppm K ⁻¹)	E (GPa)	ϵ_b ave/max (%)	σ_b (GPa)	T_g^N (N ₂) (°C)	T_g^A (air) (°C)
TA-NBHQ	1.89 ^a	T	–	Turbid	0	–	– ^c	219 ^d 230 ^e	67.3	3.97	23/48	0.11	452	438
	2.63 ^b	C	DMAc (15.1 wt%)	Turbid	12.2	372	0.077	219 ^d 238 ^e	48.4	4.59	7/14	0.12	444	444
TA-BHQ	2.80 ^a	T	–	Turbid	0	–	– ^c	226 ^d 232 ^e	56.8	3.46	19/59	0.09	450	419
	3.24 ^b	C	DMAc (10.7 wt%)	Slightly turbid	58.7	359	0.117	234 ^d 243 ^e	10.1	5.58	15/25	0.23	489	430
TA-25DBHQ	0.95 ^a	T	–	Clear	59.6	360	0.033	272 ^d 284 ^e	57.6	3.38	8/10	0.12	441	405
	1.18 ^b	C	DMAc (15.1 wt%)	Clear	71.6	354	0.043	254 ^d 264 ^e	33.5	3.48	5/6	0.10	435	402
TA-25DAHQ	3.23 ^a	T	–	Clear	51.3	360	0.004	261 ^d 283 ^e	74.6	2.80	17/27	0.13	431	392
	5.20 ^b	C	DMAc (10.6 wt%)	Clear	70.9	362	0.027	266 ^d 270 ^e	42.6	3.48	17/23	0.15	449	404

^a Data for PAA solutions just after polymerization.

^b Data for chemically imidized powder samples. For chemical imidization, the same PAA as that for thermal imidization was used unless the data for PAA was indicated in the cell.

^c The refractive index measurements were difficult because of intensive turbidity.

^d Data determined by DMA (method-1).

^e Data determined by TMA (method-2).

imidization; it exhibited an outstandingly low CTE (10.1 ppm K⁻¹) with a comparatively high T_{400} value of 58.7%. Among all the PEI films (C and T) examined in this work, only the TA-BHQ/TFMB film (C) exhibited a sign of crystallization in the WAXD pattern.

The addition of one more *tert*-butyl group into TA-BHQ (i.e., TA-25DBHQ) was effective for further improvement of the transparency; casting from the DMAc solution led to an almost colorless PEI film with a high T_{400} (71.6%), a high T_{tot} (88.9%), and a very low YI (2.65) although a certain degree of increase in CTE was inevitable.

The TA-25DAHQ system (C) with bulkier amyl substituents displayed the highest transparency in this work as demonstrated from the following optical data: T_{400} = 70.9%, T_{tot} = 89.4%, and YI = 2.54, and Haze = 1.69% for the DMAc-cast film.

Table 4 summarizes the qualitatively evaluated solubility of the chemically imidized powder samples. TA-25DAHQ/TFMB possessed the highest solubility in this work; it was soluble even in non-amide less hygroscopic solvents at room temperature similarly to 6FDA/TFMB known as a typically soluble PI. Thus, the exceedingly bulky di-amyl groups behave like trifluoromethyl groups as a typical solubility-promoting substituent.

3.3. Influence of side group bulkiness

Fig. 7 shows how the substituents affect some important properties of the PEI films (C). Here, the bars in the column charts are roughly arranged in the order of the side group bulkiness. Getting rid of highly turbid films, a trend was observed for the T_{400} -based film transparency; the bulkier substituents seem to be favorable for enhancing the film transparency [Fig. 7 (a)]. To cancel an effect of intermolecular interactions on the transparency, the ultraviolet–visible absorption spectra in solutions were also compared for the chemically imidized soluble PEIs. The molar extinction coefficient at 400 nm (ϵ_{400} , in base M⁻¹ cm⁻¹) in GBL at room temperature increased in the following order: 3.84 (TA-TMHQ/TFMB) < 5.22 (TA-BHQ/TFMB) < 6.08 (TA-25DAHQ/TFMB) < 9.80 (TA-NBHQ/TFMB) < 13.1 (TA-MeOHQ/TFMB) < 13.7 (TA-25DBHQ/TFMB) < 15.9 (TA-26DMHQ). Actually, no clear correlation between T_{400} (film) and ϵ_{400} (in GBL) was observed (the figure is not shown here). This suggests that the enhanced film transparency with increasing substituent bulkiness results from disturbed intermolecular interactions rather than the intramolecular reason (weaker visible absorption of the isolated chains).

Table 4
The solubility of chemically imidized powder samples for homo TA-HQs/TFMB systems. The tests were carried out by adding the samples (10 mg) in solvents (1 mL).

Tetracarboxylic dianhydride	NMP	DMAc	DMF	DMSO	<i>m</i> -cresol	CPN	GBL	DOX	THF	CF	Acetone	Tri-GL
	Temperature in solubility test upon heating (°C)											
	150	150	140	150	150	130	150	100	60	50	50	150
TA-MHQ	+	+	+	–	–	–	–	–	–	–	–	–
TA-MeOHQ	+	+	+	+	+	+	+	±	–	–	–	–
TA-26DMHQ	++	++	+ ^a	+ ^a	+	+	+	+	++	+	–	–
TA-TMHQ	+	+	+	+	+	+ ^a	+	+	+	–	±	–
TA-NBHQ	+	+	+	+	+	+	+	±	–	–	–	–
TA-BHQ	+ ^a	+ ^a	+ ^b	+ ^b	+	+ ^b	+ ^b	–	–	–	±	–
TA-25DBHQ	+	+	+	+	+	+ ^b	+	+	+	+	–	+
TA-25DAHQ	++	++	++	+ ^b	+	+ ^b	+ ^b	++	++	++	±	+
6FDA	++	++	++	++	+	+	++	++	++	–	++	++

(++) Soluble at room temperature, (+) soluble upon heating at established temperatures, (±) deformed or swelled, and (–) insoluble. DOX = 1,4-dioxane, CF = chloroform.

^a Gelation after the hot homogeneous solution was kept at room temperature for a few days.

^b Gelation after the hot homogeneous solution was kept at room temperature for a few hours.

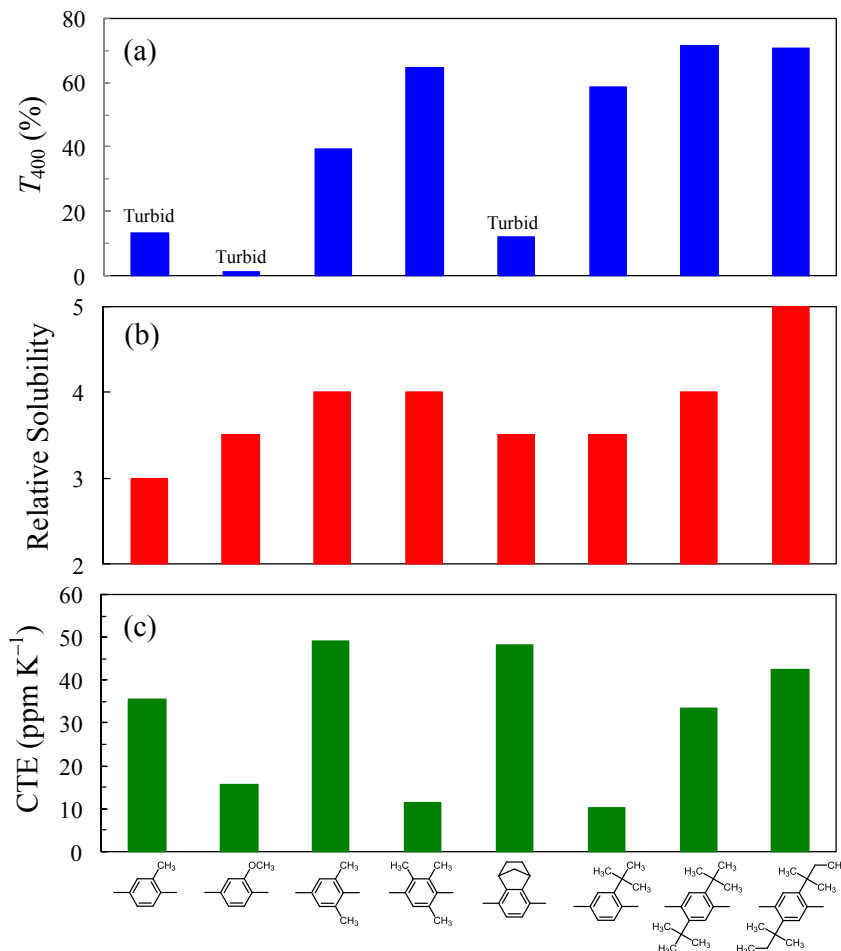


Fig. 7. Influence of side group bulkiness on some properties for chemically imidized PEIs: (a) T_{400} for PEI films, (b) relative level of solubility (5-step evaluation, see Table 7), and (c) CTE.

Prior to discussion on the solubility in Fig. 7(b), we show the qualitatively tested solubility of the PEI powder samples (C) in various solvents (Table 4). In general, amide solvents have powerful dissolution ability for common PIs, whereas less polar solvents such as ether solvents (e.g., Tri-GL) are often far away from good solvents. In this table, the solvents used are roughly arranged in the order of the dissolution ability. The results revealed that the present PEIs (C) are essentially soluble in a variety of solvents. It is obvious that the incorporation of bulkier substituents appreciably improves the solubility as illustrated typically in TA-25DAHQ/TFMB. In this work, the solubility was ranked on the basis of a criterion (see Table 7). Indeed, the solubility level gradually is enhanced with increasing side group bulkiness as illustrated in Fig. 7(b). Accordingly, this effect can be also interpreted in terms of the weakened intermolecular interactions accompanied with an increase in the substituent bulkiness.

An influence of the substituents on CTE is depicted in Fig. 7(c). In contrast to the relatively clear trends of the transparency and the solubility, no monotonous change was observed for CTE. However, there seems to be some appropriate/favorable bulkiness (or molecular shape?) of the substituents for reducing CTE. Consequently, the diamyl and di-*tert*-butyl substituents were too bulky to promote the casting-induced in-plane orientation effect.

Fig. 8 accounts for the substituent bulkiness effect on CTE and T_g for the thermally imidized PEIs. As depicted in Fig. 8(b), the CTE almost monotonously increased as the substituents become bulkier

in contrast to the chemically imidized systems. The results are consistent with a negative impact of substituents as observed in our previous work [31]; the PI system derived from *s*-BPDA and 2,5-dimethyl-1,4-phenylenediamine (DMPDA) with excessive alkyl substituents showed no significant in-plane orientation behavior upon thermal imidization in contrast to the non-substituted counterpart (*s*-BPDA/*p*-PDA). The results of Fig. 8(b) probably imply that the combination of backbone linearity/stiffness and intimate interchain stacking is indispensable for reducing CTE upon thermal imidization. It is reasonable to assume that the increase in the substituent bulkiness disturbs dense chain stacking, consequently weakens interchain interactions. On the basis of this consideration, a gradual decrease in T_g [Fig. 8(a)] can be explained without contradiction.

3.4. In-plane orientation behavior quite different by imidization methods

As described above, it is undoubted that CTE is primarily dominated by the degree of in-plane orientation in the PEI films [see Fig. 5(a)]. For further improvement of thermal expansion property, it is important to examine how the in-plane orientation proceeds concomitantly with solvent evaporation from the coated PEI solutions on substrates. Fig. 9 depicts a schematic illustration for an in-plane orientational change during the film formation by simple drying of a coated PEI solution (solid line). For a

Table 5
Film properties of TA-25DBHQ/TFMB-based copolymer systems.

Comonomer (mol%)	η_{inh} (dL g ⁻¹)	Cure	Solvent (PI content)	Appearance of PI films	T_{400} (%)	λ_{cut} (nm)	Δn_{th}	T_g (°C)	CTE (ppm K ⁻¹)	E (GPa)	ϵ_b ave/max (%)	σ_b (GPa)	T_d^5 (N ₂) (°C)	T_d^5 (air) (°C)	W_A (%)
Homo PEsl	0.95 ^c	C	DMAc (15.1 wt%)	Clear	71.6	354	0.043	254 ^e	33.5	3.48	5/6	0.10	435	402	
PMDA (0)	1.18 ^d							264 ^f							
PMDA (30)	1.79 ^c	T	—	Turbid	2.2	386	0.018	257 ^e	50.4	3.84	9/16	0.13	439	408	
Random ^a	3.80 ^d	C	CPN (7.0 wt%)	Clear	50.9	365	0.096	272 ^e	13.0	5.21	11/22	0.18	461	421	0.04
								298 ^f							
PMDA (30)	2.42 ^c	C	CPN (6.1 wt%)	Clear	50.1	365	0.097	257 ^e	12.1	4.98	11/16	0.18	465	422	0.08
SC ^b	6.25 ^d							295 ^f							
PMDA (40)	2.14 ^c	C	CPN (8.0 wt%)	Clear	35.3	369	0.104	273 ^e	8.6	5.23	12/22	0.21	472	428	
Random								292 ^f							
s-BPDA (30)	2.02 ^c	C	CPN (10.8 wt%)	Clear	66.6	369	0.091	266 ^e	18.0	4.36	12/21	0.16	463	430	
Random	4.19 ^d							282 ^f							
s-BPDA (50)	1.01 ^c	T	—	Clear	52.8	374	0.003	295 ^e	56.0	3.64	13/25	0.14	444	412	
Random	1.77 ^d	C	DMAc (8.6 wt%)	Clear	63.8	372	0.061	263 ^e	33.1	4.34	12/19	0.16	484	432	
								310 ^f							
TA-HQ (50)	1.44 ^c	C	CPN (8.3 wt%)	Turbid	62.1	358	0.107	237 ^e	17.1	5.26	9/17	0.17	483	427	
Random	2.53 ^d							257 ^f							
NTDA (30)	1.49 ^c	C	CPN (8.2 wt%)	Clear	58.1	383	0.116	290 ^e	7.4	5.26	8/13	0.17	468	432	
Random	3.27 ^d							302 ^f							
TA-BHQ (50)	1.11 ^c	C	CPN (13.8 wt%)	Clear	70.1	358	0.071	247 ^e	25.2	3.88	9/14	0.14	460	419	0.08
Random	1.71 ^d							255 ^f							
TA-BHQ (70)	2.19 ^c	C	CPN (7.8 wt%)	Clear	69.5	357	0.098	245 ^e	20.5	4.77	18/37	0.18	426	418	0.10
Random	3.95 ^d							253 ^f							
TA-TMHQ (50)	2.79 ^c	C	CPN (8.1 wt%)	Clear	57.8	363	0.085	270 ^e	16.1	4.18	13/24	0.19	454	418	
Random								278 ^f							
TA-TMHQ (70)	2.62 ^c	C	CPN (8.7 wt%)	Clear	63.2	361	0.091	264 ^e	18.2	4.58	18/35	0.21	458	421	
Random								278 ^f							

^a Random copolymerization was carried out by adding mixed powder of tetracarboxylic dianhydrides into TFMB solution.

^b Sequence-controlled (SC) copolymerization was carried out by first adding TA-25DBHQ powder into TFMB solution, stirring 24 h, then adding PMDA powder.

^c Data for PAA solutions just after polymerization.

^d Data for chemically imidized powder samples. For chemical imidization, the same PAA as that for thermal imidization was used unless the data for PAA was indicated in the cell.

^e Data determined by DMA (method-1).

^f Data determined by TMA (method-2).

comparison, the case of conventional two-step process (PAA casting and successive thermal imidization, broken lines) is overlaid on this figure. First, we mention the orientational behavior for the PI films (T). An initial strategy for reducing CTE was to investigate the structure–CTE relationship [32–34]. In order to fully understand

the principle of low CTE generation, initial interests have been directed to a role of thermal imidization on the in-plane chain alignment [31,35]. In particular, the s-BPDA/p-PDA system has thoroughly been investigated since it is a practically useful heat-resistant material with a very low CTE. Some experimental

Table 6
Film properties of TA-25DAHQ/TFMB-based copolymer systems prepared via chemical imidization.

Comonomer (mol%)	η_{inh} (dL g ⁻¹)	Solvent (PI content)	T_{400} (%)	λ_{cut} (nm)	Δn_{th}	T_g (°C)	CTE (ppm K ⁻¹)	E (GPa)	ϵ_b ave/max (%)	σ_b (GPa)	T_d^5 (N ₂) (°C)	T_d^5 (air) (°C)	W_A (%)
Homo PEsl	3.23 ^a	DMAc (10.6 wt%)	70.9	362	0.027	266 ^d	42.6	3.48	17/23	0.15	449	404	
PMDA (0)	5.20 ^b					270 ^e							
PMDA (30)	3.65 ^a	CPN (6.9 wt%)	46.3	368	0.096	280 ^d	14.7	4.82	10/22	0.17	454	415	0.08
Random	9.82 ^b		57.3 ^c			289 ^e							
PMDA (40)	2.37 ^a	Tri-GL (5.3 wt%)	49.6	363	0.086	269 ^d	13.2	4.86	11/25	0.18	452	410	
Random						294 ^e							
s-BPDA (30)	4.82 ^a	CPN (7.2 wt%)	64.5	370	0.096	262 ^d	19.1	4.06	13/20	0.17	430	423	0.09
Random	17.7 ^b					280 ^e							
s-BPDA (50)	2.75 ^a	DMAc (8.9 wt%)	65.0	372	0.092	270 ^d	20.4	4.50	14/23	0.18	465	436	0.06
Random	6.56 ^b					284 ^e							
NTDA (30)	2.19 ^a	CPN (9.1 wt%)	53.1	383	0.081	275 ^d	15.8	3.49	15/28	0.15	481	405	0.31
Random	3.21 ^b					290 ^e							
TA-25DBHQ (25)	1.92 ^a	Tri-GL (9.0 wt%)	69.1	359	0.051	262 ^d	34.8	3.38	12/23	0.14	401	398	0.11
Random	3.57 ^b					266 ^e							
TA-25DBHQ (50)	3.30 ^a	Tri-GL (9.2 wt%)	71.1	358	0.063	260 ^d	27.7	3.70	10/20	0.15	399	398	0.11
Random	6.67 ^b					269 ^e							
TA-25DBHQ (75)	3.62 ^a	Tri-GL (8.0 wt%)	70.2	355	0.063	269 ^d	27.0	3.82	10/19	0.15	441	408	0.14
Random	7.82 ^b					273 ^e							

^a Data for PAA solutions just after polymerization.

^b Data for chemically imidized powder samples.

^c Data for Tri-GL-cast PEsl film.

^d Data determined by DMA (method-1).

^e Data determined by TMA (method-2).

Table 7
Criteria for 5-step evaluation of the target properties.

Properties	Parameters	Relative level				
		1	2	3	4	5
Transparency (Tr)	T_{400} (%)	<5	20–30	40–60	70–75	>80
Low thermal expansion property (LT)	CTE (ppm K ⁻¹)	>70	60–50	45–35	30–20	<10
Heat resistance (HR)	T_g (°C) ^a	<200	220–240	250–270	280–300	>350
Toughness (To)	ϵ_b^{\max} (%)	No film-forming ability or <2	5–10	20–30	40–60	>100
Solution-processability (SP)	Qualitative solubility	Insoluble upon heating	Partially soluble or swelled	Soluble in hot amide solvents	Soluble in amide solvents at r.t. or hot ether solvents	Soluble in various non-amide solvents at r.t.

Samples soluble in hot CPN or hot GBL: SP-level = 3.5.

^a Data determined by DMA (method-1).

evidence suggests that the in-plane orientation for *s*-BPDA/*p*-PDA proceeds as depicted in Fig. 9(b) (1T) in the simplified heating process [60 °C/2 h + 250 °C/2 h, Fig. 9(a)] [31]; the in-plane chain alignment is drastically enhanced in the thermal imidization process. In contrast, PI systems with flexible/distorted backbone structures (e.g., *s*-BPDA/4,4'-ODA) undergo orientational relaxation upon thermal imidization [Fig. 9 (2T)]. On the other hand, in a system where the backbone itself remains rigid but with excessive alkyl substituents (e.g., *s*-BPDA/DMPDA), the in-plane orientation increases only slightly upon thermal imidization [Fig. 9 (3T)]. A similar situation is also observed in the present TA-TMHQ/TFMB system (T) as suggested from its high CTE (54.3 ppm K⁻¹, Table 2).

However, chemical imidization of TA-TMHQ/TFMB swept away a reputation as a “worthless material” as stated above; the curve (3C) represents that the PEI chains for TA-TMHQ/TFMB can highly align

along the film plane just by drying at 60 °C for 2 h. Then, the half-dried PEI film obtained probably undergoes additional orientational enhancement by fully drying it on the substrate at 250 °C owing to an expected apparent stretching effect concomitant to a slight thickness decrease as mentioned later. This hypothesis is based on our previous observation; i.e., melt-induced in-plane orientation behavior by annealing above the T_g on the substrates for *s*-BPDA/TFMB [36]. Indeed, the substrates must play a great role when annealed at 250 °C in the present case; if the substrate was removed after drying at 60 °C for 2 h, the half-dried TA-TMHQ/TFMB PEI film most likely suffers somewhat orientational relaxation by heating at 250 °C (3C') as suggested from the fact that CTE = 13.0 ppm K⁻¹ in case of heating on the substrate and CTE = 22.3 ppm K⁻¹ off substrate for TA-25DBHQ(70); PMDA(30)/TFMB copolymer.

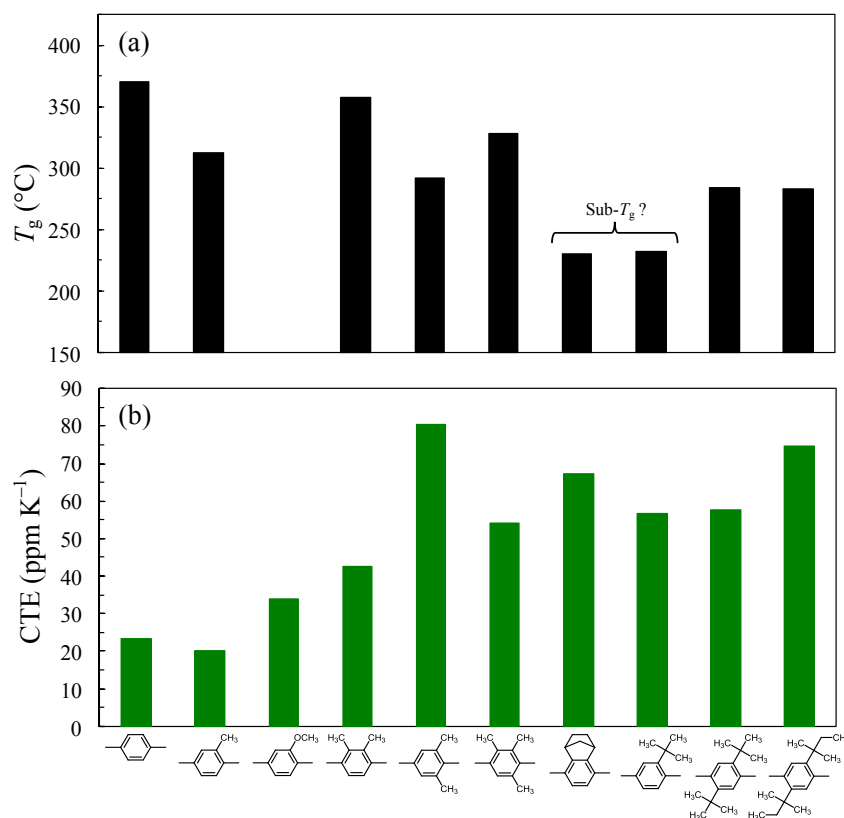


Fig. 8. Influence of side group bulkiness on some properties for thermally imidized PEIs: (a) T_g by TMA (method-2) and (b) CTE.

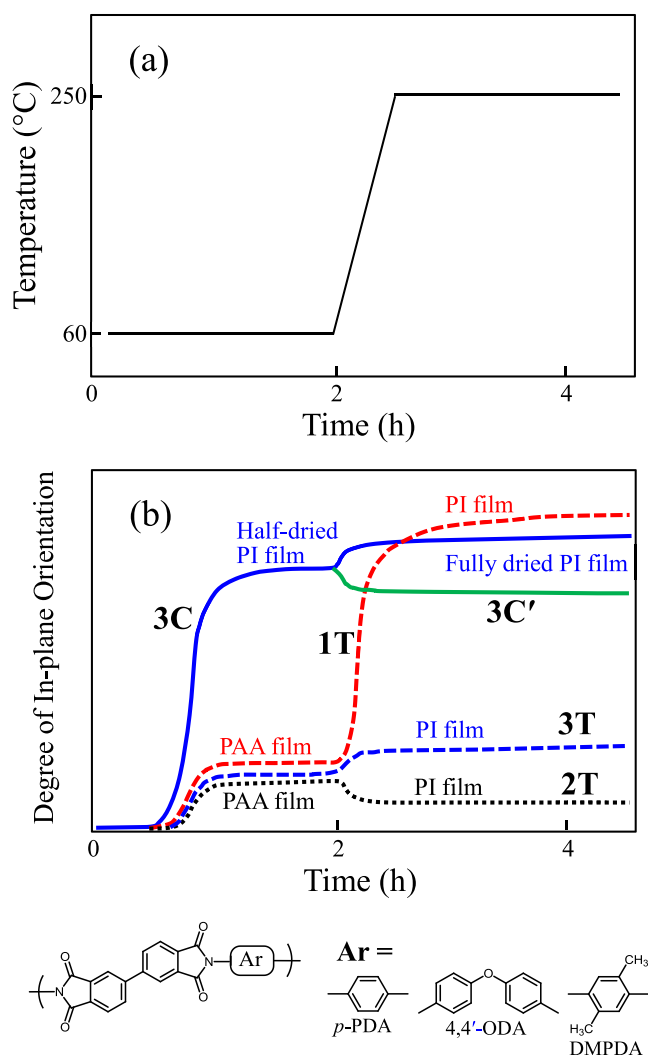


Fig. 9. Changes in coating, drying, and heat treatment processes: (a) simplified temperature profile and (b) presumed changes in the degree of in-plane orientation during thermal imidization (broken lines, 1T: *s*-BPDA/*p*-PDA, 2T: *s*-BPDA/4,4'-ODA, 3T: *s*-BPDA/DMPDA) or TA-TMHQ/TFMB and solution casting of chemically imidized PEIs (solid lines, 3C: TA-TMHQ/TFMB on substrate, and 3C': TA-TMHQ/TFMB off substrate after drying at 60 °C for 2 h).

Both of the present system (3C) and the conventional system (1T) finally bring out low CTE. However, the shape of the curve (i.e., orientational behavior) for the former is quite different from that for the latter. It is undoubted that the thermal imidization reaction for the latter acts as a trigger for the orientational enhancement. The trigger is attributed to an “apparent stretching” effect, which generates by inhibiting significant film contraction on the substrate [31]. On the other hand, there seems to be no distinguished driving force appropriate for the actual pronounced in-plane orientation in the sample (3C); although there must be another type of stretching effect accompanied with thickness decrease during solvent evaporation as described in our previous paper [16] (see [Supplementary data 3](#)), it is probably too weak as the driving force as inferred from our experience that simple casting from an NMP solution of PES caused no appreciable in-plane orientation (almost zero Δn_{th}). Therefore, other effective driving forces should be considered to account for the curious phenomenon in the sample (3C). A possible idea assumes the presence of some local ordered structure ([Supplementary data 3](#)), which is favorably formed when the main

chains are highly linear/rigid. This hypothesis is based on our previous observation; a liquid crystal-like ordered structure at the PAA stage obviously contributes to a decrease in CTE [37]. If such a local ordered structure (maybe undetectable on a polarizing optical microscope) could be formed with solvent evaporation prior to solidification in the present systems, it is likely that the in-plane orientation is intensified cooperatively with the subsequent weak stretching effect.

Thus, the chain orientation mechanism in the film formation process (3C) seems to be quite different from that in the process (1T). However, in this work we tried to find out some common feature between them from the viewpoint of “molecular mobility” during the film formation processes. Our previous studies revealed that the degree of in-plane orientation is affected by some structural factors (backbone linearity/stiffness) and processing conditions (heating rate, film thickness, solvents and amounts of residual solvents in PAA films) during thermal imidization [31,36]. It is accepted that the residual amide solvents behave as a plasticizer [38]. Accordingly, the following factors can be regarded to be equivalent in terms of “molecular mobility” during thermal imidization: (increases in imidization temperature, heating rate, film thickness, and residual solvent content, and a decrease in solvent volatility). [Fig. 10\(a\)](#) schematically depicts the in-plane orientational behavior affected by molecular mobility during thermal imidization, although actual situation is much more complicated

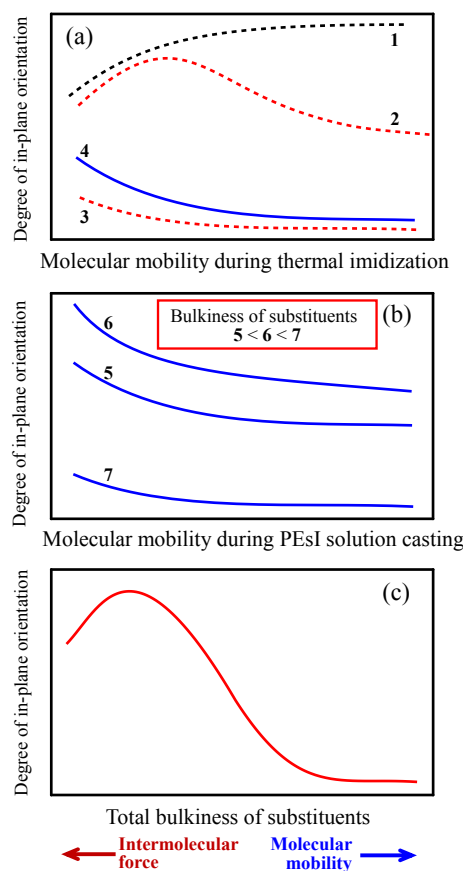


Fig. 10. Schematic diagrams for the degree of in-plane chain orientation as influenced by some factors: (a) molecular mobility during thermal imidization of PAA films, (b) molecular mobility during solution casting of chemically imidized PEIs, and (c) total bulkiness of substituents in the present PEIs. 1: PMDA/*p*-PDA, 2: *s*-BPDA/*p*-PDA, 3: *s*-BPDA/4,4'-ODA, 4: *s*-BPDA/DMPDA or TA-TMHQ/TFMB, 5: TA-MHQ/TFMB, 6: TA-TMHQ/TFMB, 7: TA-25DAHQ/TFMB.

because of significantly varying molecular mobility with the progress of imidization. Rod-like PI systems (e.g. PMDA/*p*-PDA), which is unfavorable in terms of molecular mobility, should be prepared under severer conditions (for example, at higher imidization temperatures or with higher heating rates) for maximizing the in-plane orientation. On the contrary, flexible PI systems (e.g., *s*-BPDA/4,4'-ODA) prefer milder imidization conditions to suppress orientational relaxation. On the other hand, the in-plane orientation can be maximized under a thermal imidization condition with a medium intensity of molecular mobility for semi-rigid PI systems (e.g., *s*-BPDA/*p*-PDA). Thus, such optimum intensity of the molecular mobility for maximizing the in-plane orientation shifts with the backbone linearity/stiffness.

On the other hand, we also found out some factors advantageous for enhancing the in-plane orientation by simple casting of PI solutions, i.e., the increases in PI molecular weights, solvent volatility, and the decreases in drying temperature and heating rate [16]. The results suggest that the in-plane orientation tends to increase with decreasing molecular mobility during solution casting (under milder conditions). Therefore, the in-plane orientation can be roughly represented as a monotonously decreasing curve with increasing molecular mobility [Fig. 10(b)], although the actual curve may possess a “peak” at a low molecular mobility. This figure also reflects the results of the present PEI systems with three different substituents (mono-methyl, tri-methyl, and di-amyl groups). Fig. 10(c) suggests the presence of an optimum substituent size for maximizing the casting-induced in-plane orientation. Assuming that an increase in the substituent bulkiness corresponds to a decrease in intermolecular forces, in other words, an increase in molecular mobility during the casting process, there seems to be a roughly common feature in the in-plane orientation behavior even when the films were prepared via different routes [see the curve in Fig. 10(c) and curve 2 in Fig. 10(a)]. Thus, seeking out an optimum condition from the viewpoint of molecular mobility must be the strategy common to the different imidization methods (C and T).

3.5. Property improvement by copolymerization

3.5.1. TA-25DBHQ/TFMB-based copolymers

As described above, the pronounced feature of the TA-25DBHQ/TFMB system (C) is outstanding transparency although there is room for further improvement of the thermal expansion property (CTE = 33.5 ppm K⁻¹). Copolymerization using some rigid tetracarboxylic dianhydrides with a minor fraction may contribute to a decrease in the CTE while avoiding significant deterioration of the transparency. Table 5 summarizes the film properties of TA-25DBHQ/TFMB-based copolymer systems.

Our first attempt was to copolymerize using PMDA known as the most familiar rigid tetracarboxylic dianhydride, which is based on the fact that the homo PMDA/TFMB system brings about a considerably low CTE upon thermal imidization [17,39]. Against our expectation, no significant effect on CTE was observed by random copolymerization (PMDA = 30 mol%) when the film was prepared via thermal imidization. This probably reflects too high molecular mobility during thermal imidization in this copolymer, which arises from weakened intermolecular force by the bulky substituents (di-*tert*-butyl groups), thereby orientational relaxation becomes preferential. The PMDA-modified copolymer film (T) was also poorly transparent. However, in contrast to such worthless results, the chemically imidized counterpart exhibited a significantly decreased CTE (13.0 ppm K⁻¹) while maintaining relatively high transparency. The suppressed water uptake is also another feature of this system, which probably results from the presence of hydrophobic substituents (CF₃ and the di-*tert*-butyl groups). It should be noted that the solubility of the powder sample (C) was obviously

improved by using PMDA comonomer (see Supplementary data 4) against our initial concern coming from the fact that homo PMDA/TFMB is essentially insoluble. As expected, an increase in the PMDA content to 40 mol% further decreased the CTE, but it also caused inevitably a significant deterioration in the transparency.

The control of chain sequence occasionally brings about a positive effect on some properties. For example, sequence-controlled copolymerization consisting of PMDA, 4,4'-ODA, and *p*-PDA provides lower CTE and higher ϵ_b than the corresponding random copolymers [40]. Besides, a siloxane-containing block-like copolymer produces a much lower modulus than the corresponding random copolymer [41]. Such technique was also applied to the present copolymer system. Unfortunately, the effect of sequence control was not so pronounced at a PMDA content of 30 mol% (Table 5).

s-BPDA was also used as another comonomer. The copolymer film (C) at *s*-BPDA = 30 mol% afforded well-balanced properties; a low CTE (18.0 ppm K⁻¹) close to that of copper foil and relatively high transparency ($T_{400} = 66.6\%$), although the modification effect got inconspicuous at *s*-BPDA = 50 mol%. A similar positive copolymerization effect was also observed by using TA-HQ comonomer. On the other hand, it should be noted that the modification using NTDA (30 mol%) is capable of drastically decreasing the CTE (7.4 ppm/K) and significantly increasing the T_g (290 °C) while maintaining excellent solubility (see Supplementary data 4) and good transparency, which is obviously higher than for the corresponding PMDA-modified copolymer.

The copolymer systems modified with conventional rigid monomers (PMDA, *s*-BPDA, and NTDA) showed a CTE- Δn_{th} curve different from that of the homo substituted TA-HQs/TFMB as depicted in Fig. 5 (a). The downward-shifted curve for the copolymers may imply that these conventional rigid monomers have distinctly greater ability for enhancing the in-plane orientation than the substituted TA-HQs.

As mentioned above, two homo PEI systems (C), i.e., TA-BHQ/TFMB and TA-TMHQ/TFMB possess considerably low CTE values (~10 ppm K⁻¹). According to the results, we also used TA-BHQ and TA-TMHQ as comonomers for improving the insufficient thermal expansion property of TA-25DBHQ/TFMB; they were copolymerized with a high content of 50 or 70 mol%. This approach was also effective for affording well-balanced properties with respect to low CTE and high transparency. In particular, the modification using TA-BHQ is superior in the transparency to that with TA-TMHQ; the former is capable of lowering the CTE without practical deterioration of the transparency as shown in Table 5.

Besides, among the TA-25DBHQ/TFMB-based copolymer systems (C), the solubility was most effectively enhanced when *s*-BPDA was used as a property modifier (see Supplementary data 4).

3.5.2. TA-25DAHQ/TFMB-based copolymers

The predominant feature of TA-25DAHQ/TFMB (C) is its distinguished solubility in addition to its outstanding transparency. Because of the excellent solubility, solution casting can be made even by means of Tri-GL with a much lower dissolution power than amide solvents. Empirically speaking, the film coloration also depends on casting solvents, and it tends to increase in the following order: Tri-GL < CPN < DMAc << NMP. Therefore, the Tri-GL-process compatibility has great superiority in enhancing the transparency.

The properties of TA-25DAHQ/TFMB-based copolymers are summarized in Table 6. For the TA-25DAHQ/TFMB copolymer modified with 30 mol% PMDA, solution casting using CPN caused a significantly decreased CTE although the transparency ($T_{400} = 46.3\%$) somewhat deteriorated. On the other hand, the use of Tri-GL instead of CPN improved indeed the transparency ($T_{400} = 57.3\%$). Even when the PMDA content was increased to

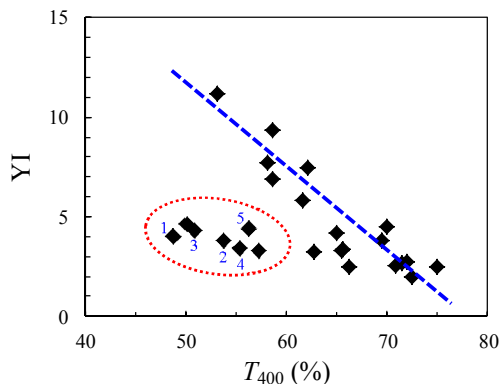


Fig. 11. Correlation between T_{400} and YI: (1) TA-25DAHQ(70);PMDA(30)/TFMB, (2) TA-25DAHQ(60);PMDA(40)/TFMB, (3) TA-25DBHQ(70);PMDA(30)/TFMB (random), (4) TA-25DBHQ(70); s-BPDA(30)/TFMB, and (5) TA-25DBHQ(50); s-BPDA(50)/TFMB.

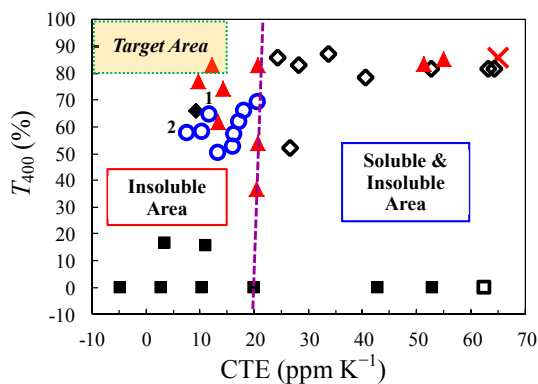


Fig. 12. CTE–transparency–solubility diagram: (\circ) some selected systems of this work, 1: TA-TMHQ/TFMB and 2: TA-25DBHQ(70); NTDA(30)/TFMB], (\diamond , \square) soluble PIs, (\blacksquare , \blacktriangle , \blacklozenge) insoluble PIs, (\times) PES. Open and closed symbols denote soluble and insoluble materials, respectively.

40 mol%, the copolymer system could be processed using Tri-GL owing to the originally outstanding solubility of the pristine TA-25DAHQ/TFMB system.

Modifications using s-BPDA and NTDA comonomers produced well-balanced properties (low CTE, maintained transparency, very low amounts of water absorption, and sufficient ϵ_b , Table 6) without sacrificing the solubility (see Supplementary data 5).

The copolymerization approach also produced another positive effect on film yellowness control. A linear relationship is roughly observed between T_{400} and YI as depicted in Fig. 11. It should be noted that some of the data points for the TA-25DAHQ/TFMB-based copolymers with minor fraction of PMDA or s-BPDA (surrounded by broken circle) deviate distinctly downward from the YI– T_{400} correlation (broken line). This implies that the use of these rigid comonomers with minor fractions was very effective to restrain the film yellowing although the discernible decreases in T_{400} were actually inevitable as mentioned above. A similar effect was also observed for TA-25DBHQ/TFMB-based copolymers. The unexpectedly suppressed film yellowness for these copolymers is closely related to the absence of a weak absorption band (tail) in the wavelength range (420–480 nm), which corresponds to the complementary colors of yellow [19].

3.6. Position of our PEIs as low-CTE transparent materials and performance balance

Fig. 12 displays a CTE–transparency–solubility diagram, which stands for the status of our PEIs with respect to the practical use. The target area (CTE ≤ 15 ppm K^{-1} and $T_{400} \geq 80\%$) is also indicated in this figure. PES and all other conventional colorless engineering plastics are removed from the present candidates because of their too high CTE. Most of conventional or previously reported colorless PIs (e.g., 6FDA/TFMB and cycloaliphatic PIs) possess no satisfactorily low CTE [13–15,18,19]. A general trend is observed in this figure; conventional PIs abruptly lose the transparency and the solubility below CTE ~ 20 ppm K^{-1} as typically in the s-BPDA/*p*-PDA system. The s-BPDA/*t*-CHDA system is a limited case possessing high transparency and low CTE [29]. However, its essential insolubility prevents us from applying the chemical imidization process. On the other hand, it should be noted that our PEIs (\circ , Fig. 12) was capable of escaping from such general tendency and simultaneously accomplished low CTE, high transparency, and excellent solution-processability. For example, the data points for TA-TMHQ/TFMB (#1) and TA-25DBHQ(70); NTDA(30)/TFMB (#2) are located

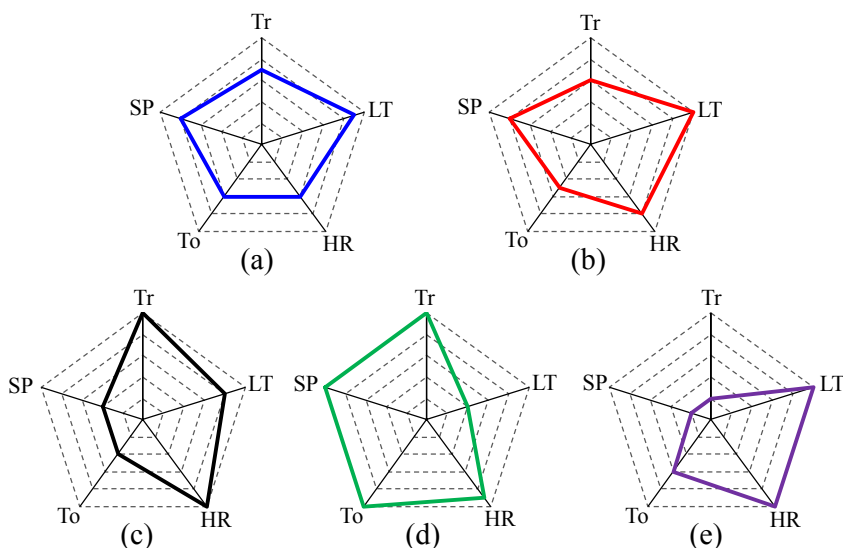


Fig. 13. Performance balance represented by 5-level evaluation for the systems derived from TFMB with different tetracarboxylic dianhydrides: (a) TA-TMHQ, (b) TA-25DBHQ(70); NTDA(30), (c) CBDA, (d) 6FDA, and (e) PMDA. The criteria and abbreviations of the properties are shown in Table 7.

near the target area as indicated in Fig. 12.

We also compared performance balance for our PEIs with that for other conventional TFMB-derived systems. The properties were evaluated with five levels on the basis of criteria listed in Table 7. As depicted in Fig. 13, the spider chart for CBDA/TFMB is expanded biasedly on the right side owing to the absence of solution-processability and film toughness. The 6FDA/TFMB system almost fulfills the present target properties except for the low CTE characteristics. PMDA/TFMB also gives a significantly deformed spider chart because it does not satisfy the required properties except for the low-CTE and high- T_g characteristics. The results manifest how it is difficult to actualize good performance balance for the required properties. On the other hand, it is obvious that TA-TMHQ/TFMB, as well as TA-25DBHQ(70); NTDA(30)/TFMB copolymer, has an outstandingly well-balanced performance.

4. Conclusions

A series of PEIs (TA-HQs/TFMB) with various alkyl substituents were prepared for applications as novel plastic substrate materials in image display devices. A significant impact of the substituent bulkiness on the CTE and the other important properties was observed in this work. We found out some promising candidate systems on systematic investigations. For example, the chemically imidized TA-TMHQ/TFMB was soluble even in non-amide solvents such as CPN. Simple casting process from the CPN solution afforded a flexible and less colored film with a considerably low CTE (11.5 ppm K^{-1}), a high T_g of $276 \text{ }^\circ\text{C}$ (by TMA), high thermal stability (5% weight loss temperature in N_2 : $453 \text{ }^\circ\text{C}$), and very suppressed water uptake ($W_A = 0.13\%$). The low CTE results from a high extent of in-plane chain orientation, which took place during solvent evaporation after the PEI solution was coated on a substrate. On the other hand, thermally imidized counterpart was worthless in terms of low CTE and high transparency.

The copolymerization approach using conventional rigid tetracarboxylic dianhydrides as comonomers was very effective for further improving the thermal properties of PEI systems (C) including bulky substituents. For example, copolymerization of NTDA (30 mol%) to TA-25DBHQ/TFMB caused not only a drastic decrease in the CTE (7.4 ppm K^{-1}) but also an enhancement of the T_g ($290 \text{ }^\circ\text{C}$) while keeping good transparency and excellent solution-processability. This approach was also very effective to restrain the film yellowness. Thus, some of the PEIs developed in this work can be applied as novel plastic substrate materials.

Acknowledgments

We are indebted to Mr. S. Tsukuda for his partial experimental support.

Appendix A. Supplementary data

Supplementary data related to this article can be found at <http://dx.doi.org/10.1016/j.polymer.2015.07.026>.

References

- [1] M.I. Bessonov, M.M. Koton, V.V. Kudryavtsev, L.A. Laius (Eds.), *Polyimides: Thermally Stable Polymers*, Plenum, New York, 1987.
- [2] M.I. Bessonov, V.A. Zubkov (Eds.), *Polyamic Acid and Polyimides: Synthesis, Transformation and Structure*, CRC Press, Boca Raton, FL, 1993.
- [3] S. Ando, M. Ueda, M. Kakimoto, M. Kochi, T. Takeichi, M. Hasegawa, R. Yokota (Eds.), *The Latest Polyimides: Fundamentals and Applications*, second ed., NTS, Tokyo, 2010.
- [4] C.E. Sroog, *Prog. Polym. Sci.* 16 (1991) 561–694.
- [5] M. Hasegawa, K. Horie, *Prog. Polym. Sci.* 26 (2001) 259–335.
- [6] H. Suzuki, T. Abe, K. Takaishi, M. Narita, F. Hamada, *J. Polym. Sci. Part A* 38 (2000) 108–116.
- [7] W. Volksen, H.J. Cha, M.I. Sanchez, D.Y. Yoon, *React. Funct. Polym.* 30 (1996) 61–69.
- [8] T. Matsumoto, T. Kurosaki, *Macromolecules* 30 (1997) 993–1000.
- [9] T. Matsumoto, *Macromolecules* 32 (1999) 4933–4939.
- [10] H. Seino, T. Sasaki, A. Mochizuki, M. Ueda, *High Perform. Polym.* 11 (1999) 255–262.
- [11] J. Li, J. Kato, K. Kudo, S. Shiraishi, *Macromol. Chem. Phys.* 201 (2000) 2289–2297.
- [12] A.S. Mathews, I. Kim, C.S. Ha, *Macromol. Res.* 15 (2007) 114–128.
- [13] M. Hasegawa, K. Kasamatsu, K. Koseki, *Eur. Polym. J.* 48 (2012) 483–498.
- [14] M. Hasegawa, D. Hirano, M. Fujii, M. Haga, E. Takezawa, S. Yamaguchi, A. Ishikawa, T. Kagayama, *J. Polym. Sci. Part A* 51 (2013) 575–592.
- [15] M. Hasegawa, M. Horiuchi, K. Kumakura, J. Koyama, *Polym. Int.* 63 (2014) 486–500.
- [16] M. Hasegawa, M. Fujii, J. Ishii, S. Yamaguchi, E. Takezawa, T. Kagayama, A. Ishikawa, *Polymer* 55 (2014) 4693–4708.
- [17] M. Hasegawa, S. Horii, *Polym. J.* 39 (2007) 610–621.
- [18] T. Matsuura, Y. Hasuda, S. Nishi, N. Yamada, *Macromolecules* 24 (1991) 5001–5005.
- [19] M. Hasegawa, T. Ishigami, J. Ishii, K. Sugiura, M. Fujii, *Eur. Polym. J.* 49 (2013) 3657–3672.
- [20] S. Ando, T. Matsuura, S. Sasaki, *Polym. Prepr. Jpn.* 41 (1992) 957.
- [21] M. Hasegawa, K. Koseki, *High Perform. Polym.* 18 (2006) 697–717.
- [22] M. Hasegawa, Y. Tsumijima, K. Koseki, T. Miyazaki, *Polym. J.* 40 (2008) 56–67.
- [23] M. Hasegawa, Y. Sakamoto, Y. Tanaka, Y. Kobayashi, *Eur. Polym. J.* 46 (2010) 1510–1524.
- [24] J.C. Coburn, P.D. Soper, B.C. Auman, *Macromolecules* 28 (1995) 3253–3260.
- [25] T. Matsuura, M. Ishizawa, Y. Hasuda, S. Nishi, *Macromolecules* 25 (1992) 3540–3545.
- [26] S.H. Lin, F. Li, S.Z.D. Cheng, F.W. Harris, *Macromolecules* 31 (1998) 2080–2086.
- [27] T. Kikuchi, K. Uejima, H. Sato, *Polym. Prepr. Jpn.* 40 (1991) 3748–3750.
- [28] S. Uchimura, T. Kikuchi, T. Saito, H. Sato, M. Kojima, D. Makino, *Japanese Patent, JP-2549793B*.
- [29] M. Hasegawa, M. Koyanaka, *High Perform. Polym.* 15 (2003) 47–64.
- [30] M. Hasegawa, T. Honda, S. Kurokawa, K. Shindo, J. Ishii, *Polym. Prepr. Jpn.* 61 (2012) 4120.
- [31] M. Hasegawa, T. Matano, Y. Shindo, T. Sugimura, *Macromolecules* 29 (1996) 7897–7909.
- [32] S. Numata, S. Oohara, K. Fujisaki, J. Imaizumi, N. Kinjo, *J. Appl. Polym. Sci.* 31 (1986) 101–110.
- [33] S. Numata, K. Fujisaki, N. Kinjo, *Polymer* 28 (1987) 2282–2288.
- [34] S. Numata, N. Kinjo, D. Makino, *Polym. Eng. Sci.* 28 (1988) 906–911.
- [35] J.C. Coburn, M.T. Pottiger, *Thermal curing in polyimide films and coatings*, in: M.K. Ghosh, K.L. Mittal (Eds.), *Polyimides: Fundamentals and Applications*, Marcel Dekker, New York, 1996, pp. 207–247.
- [36] J. Ishii, N. Shimizu, N. Ishihara, Y. Ikeda, N. Sensui, T. Matano, M. Hasegawa, *Eur. Polym. J.* 46 (2010) 69–80.
- [37] S. Ebisawa, J. Ishii, M. Sato, L. Vladimirov, M. Hasegawa, *Eur. Polym. J.* 46 (2010) 283–297.
- [38] M.J. Brekner, C. Feger, *J. Polym. Sci. Part A* 25 (1987) 2479–2491.
- [39] J. Ishii, A. Takata, Y. Oami, R. Yokota, L. Vladimirov, M. Hasegawa, *Eur. Polym. J.* 46 (2010) 681–693.
- [40] H. Nagano, H. Nojiri, H. Furutani, *Abstract of polymers for microelectronics, Sci. Technol. (PME'89)*, 1989, 102–103.
- [41] M. Hasegawa, K. Morita, J. Ishii, *J. Photopolym. Sci. Technol.* 23 (2010) 495–499.